JOURNAL OF Materials CHEMISTRY

Solid state metathesis routes to transition metal carbides

Artur M. Nartowski,[a] Ivan P. Parkin,*[a] Maureen MacKenzie,[b] Alan J. Craven[b] and Iain MacLeod[b]

[a]*Department of Chemistry, University College London, 20 Gordon Street, London, UK WC1H OAJ*
[b]*Department of Physics and Astronomy, University of Glasgow, Glasgow, UK G12 8QQ*

Received 5th November 1998, Accepted 12th March 1999

Flame initiated (800 °C, 10 s) or bulk thermal (2 days, 1000 °C) reactions of mixed powders of transition metal halides and CaC_2 or Al_4C_3 produce transition metal carbides (TiC, ZrC, HfC, V_8C_7, NbC, TaC, Cr_3C_2, Mo_2C and WC) in good yields. The carbides were characterised by X-ray powder diffraction, SEM/EDX, FTIR, microelemental analysis, TEM, electron diffraction and ELNES.

Introduction

Self propagating high temperature synthesis (SHS) is a rapid method for producing ceramic materials by utilising the energy given out in a chemical reaction.[1] The process, initially developed in Russia, requires minimal external heating and can produce a range of over 500 materials.[2] Typically SHS reactions are of the oxidation reduction type *via* combination of the elements [eqn. (1)].

$$M + E \rightarrow ME \quad (1)$$

We have been involved with developing a subclass of SHS reactions termed solid state metathesis (SSM) reactions.[3] These reactions involve chemical exchange of the reacting partners and are driven largely by the lattice energy of a coproduced salt [eqn. (2)]. SSM reactions are also fast, self-energetic processes producing crystalline materials of unusual microstructure.[4] An important consequence of the formation of a coproduced salt in SSM is that an effective heat brake is applied to the reaction limiting the maximum reaction temperature to that of the boiling point of the salt. Solid state metathesis reactions have been used extensively for the formation of transition,[5] main group,[6] lanthanide[7] and actinide metal nitrides[8] using a wide range of starting materials; Li_3N, Mg_3N_2, Ca_3N_2 and Ba_3N_2. These reagents formally contain nitrogen as a trianion, N^{3-}. The metathesis reactions can then be considered as a direct exchange of nitride anions with halides [eqn. (2)].

$$MCl_3 + Li_3N \rightarrow MN + 3\ LiCl \quad (2)$$

Metal carbides share many similar properties to metal nitrides.[9] Transition metal carbides have extreme microhardness, elevated melting points (TaC has the highest reported melting point of any known material; 3950 °C), brittleness, resistance to non-oxidising acids and good electrical and thermal conductivity.[10] Thus transition metal carbides combine the properties of ceramics with those of metals to form with metal nitrides and carbonitrides a unique and industrially extremely useful set of materials.

Metal carbides, especially WC, TiC, TaC and NbC are widely used in combination with appropriate binders (cobalt, nickel) to form materials known as cemented carbides or hard metals.[11] These materials are major components of structural materials and abrasives where they combine the properties of hardness and wear resistance to give outstanding cutting performance. They are found as precipitates in many metallurgical systems such as high strength low alloy (HSLA) steels. Metal carbides also have potential as diffusion barriers and catalysts.[12] Commercial manufacture of transition metal carbides exceeds 15000 tonnes annually.[11] They are traditionally synthesised by reaction of the elements at 2300 °C in a hydrogen or inert atmosphere;[11] by reaction of a metal halide with methane at 2400 °C;[10] by alumothermal reduction at 2500–3000 °C;[13] the Marston process[14] and in the case of coatings by the CVD reaction of CH_4 and MCl_n or by a PVD technique such as sputtering.[15]

Bonding in metal carbide compounds has been explained by a variety of means.[16] These include descriptions that are largely based on covalent, ionic and band structural models. Band structure calculations can explain many of the physical properties of transition metal carbides and have gained the most acceptance. Transition metal carbides are interstitial compounds with the carbons fitting in the voids of the close packed metal array.[10] Carbides of group 4 and 5 all have a predominantly fcc-NaCl structure.[17] These materials, in most cases, can tolerate non-stoichiometry in the structure through disordered carbon vacancies, for example the TiC phase is stable from $TiC_{1.00}$ to $TiC_{0.61}$. However in the case of VC_x the carbon vacancies exhibit long range order over the entire composition range forming superlattice structures. For group 6 carbides such as WC and Mo_2C non-stoichiometry is not tolerated to such a degree and the common structural type is hexagonal. Unlike nitrides where the nitride trianion is largely accepted the existence of descrete carbide tetraanions (C^{4-}) is somewhat speculative.[12] The existence of carbide tetraanions is formulated in two materials, Al_4C_3 and Be_2C, primarily on the basis that these materials react with water to form methane. Many ionic carbides have been crystallographically characterised with the acetylide dianion unit C_2^{2-}.

Formation of metal carbides by solid state metathesis reactions has not been pursued as vigorously as formation of metal nitrides, possibly because of a perceived lack of suitable ionic carbide precursors.[3,9] Here we report the formation of a wide range of metal carbides by solid state metathesis reactions. The carbide products were characterised by a suite of X-ray powder diffraction, SEM/EDX, microelemental analysis, TEM, electron diffraction and ELNES measurements.

Results and discussion

Synthesis

Reaction of Al_4C_3 with anhydrous transition metal chlorides in an evacuated ampoule in a temperature gradient of 200–1000 °C for 2 days produces transition metal carbides and aluminium trichloride (Table 1). The aluminium trichloride largely sublimed to the cooler end of the ampoule. No solid flame (also known as a thermal flash or synthesis wave) was

Table 1 X-Ray powder diffraction data from the reactions of CaC_2 and Al_4C_3 with metal halides. All materials with only one reported lattice parameter are cubic, Cr_3C_2 is orthorhombic and Mo_2C and WC are hexagonal

Reagents	Phase identified	a_{obs}[a]/nm	a_{lit}[b]/nm
$TiCl_3 + Al_4C_3$[c]	TiC	0.4332	0.4331
$ZrCl_4 + Al_4C_3$[c]	ZrC	0.4692	0.4698
$HfCl_4 + Al_4C_3$[c]	HfC	0.4639	0.4643
$VCl_3 + Al_4C_3$[c]	V_8C_7	0.4165	0.4165
$NbCl_5 + Al_4C_3$[c]	NbC	0.4468	0.4471
$TaCl_5 + Al_4C_3$[c]	TaC	0.4456	0.4456
$CrCl_3 + Al_4C_3$[c]	Cr_3C_2	0.287 ($b=0.552$, $c=1.160$)	0.282 ($b=0.553$, $c=1.147$)
$CrCl_2 + Al_4C_3$[c]	Cr_3C_2	0.287 ($b=0.553$, $c=1.166$)	0.282 ($b=0.553$, $c=1.147$)
$MoCl_3 + Al_4C_3$[c]	Mo_2C	0.3010 ($c=0.4737$)	0.3000 ($c=0.4734$)
$MoCl_5 + Al_4C_3$[c]	Mo_2C	0.3010 ($c=0.4735$)	0.3000 ($c=0.4734$)
$WCl_4 + Al_4C_3$[c]	WC	0.2905 ($c=0.2845$)	0.2906 ($c=0.2836$)
$TiI_4 + CaC_2$[d]	TiC	0.4330	0.4331
$ZrCl_4 + CaC_2$[d]	ZrC	0.4690	0.4698
$VCl_3 + CaC_2$[d]	V_8C_7	0.4165	0.4165
$NbCl_5 + CaC_2$[d]	NbC	0.4471	0.4471
$TaCl_5 + CaC_2$[d]	TaC	0.4455	0.4456
$MoCl_3 + CaC_2$[d]	Mo_2C[e]	0.3003 ($c=0.4735$)	0.3000 ($c=0.4734$)
$WCl_4 + CaC_2$[d]	WC[e]	0.2905 ($c=0.2838$)	0.2906 ($c=0.2836$)
$TiCl_3 + CaC_2$[c]	TiC	0.4330	0.4331
$ZrCl_4 + CaC_2$[c]	ZrC	0.4690	0.4698
$HfCl_4 + CaC_2$[c]	HfC	0.4632	0.4643
$VCl_3 + CaC_2$[c]	V_8C_7	0.4165	0.4165
$TaCl_5 + CaC_2$[c]	TaC	0.4451	0.4456
$WCl_4 + CaC_2$[c]	WC[f]	0.4192	0.4221

[a] ± 0.0004 nm. [b] Metal carbides are known to be non stoichiometric, the literature lattice parameters quoted are for the stoichiometric phases.[3] [c] Ampoule reaction. [d] Filament initiated reaction. [e] Minor phases W_2C and Mo were also observed. [f] Cubic WC isolated.

observed for any of the reactions utilising Al_4C_3. After trituration of the black carbide products with tetrahydrofuran, single phase metal carbides were isolated in essentially quantitative yield [eqn. (3), X = Cl; M = Hf, Zr, W: X = I; M = Ti].

$$3MX_4 + Al_4C_3 \rightarrow 3MC + 4AlX_3 \quad (3)$$

Reaction of CaC_2 with anhydrous transition metal chlorides produces transition metal carbides (Table 1). The reaction can be promoted in an evacuated ampoule at *ca.* 220–350 °C or by flame or electric filament initiation of the powder on a ceramic tile in air. In both methods the reaction proceeds by a solid flame of approximate temperature 1100 °C that moves through the material forming a composite of calcium chloride, carbon and transition metal carbide in 5–10 s. In the case of the ampoule reactions the products were typically annealed for 2 days prior to analysis. Reactions in air were not annealed and the products were isolated within ten minutes of initiation. Trituration of either mixture with methanol enabled the calcium chloride to be removed and the metal carbide to be isolated. Carbon is expected to be coproduced in the reactions [eqn. (4)].

$$MCl_3 + 3/2CaC_2 \rightarrow MC + 3/2CaCl_2 + 2C \quad (4)$$

However this was not detected by combustion microanalysis of the metal carbide products, by X-ray powder diffraction or from SEM/EDX studies. Detailed inspection of the reaction ampoule showed that some carbon was deposited on the walls of the ampoule and some was layered with the coproduced calcium chloride.

Trituration of the product to remove the co-produced salt also helped to remove free carbon (in methanol the metal carbide sank and some trace carbon floated). Perhaps in the case of the flame reactions conducted in air some of the extra coformed carbon could have formed carbon dioxide. Remarkably the reactions conducted in air did not show detectable metal oxide or metal nitride impurities.

Characterisation

Products from both the CaC_2 and Al_4C_3 reactions were analysed before and after trituration. X-Ray powder diffraction patterns before trituration showed the metal carbide and calcium or aluminium chloride. After trituration, the coproduced salt was removed to leave in most cases single phase metal carbide products (Table 1). The phases identified by X-ray diffraction indexed well and were largely identical whether Al_4C_3 or CaC_2 was used. Average crystallite sizes as assessed by X-ray line broadening[18] (ignoring possible disorder and variations in stoichiometry effects) were of the order of 30 nm (TiC, WC) to 70 nm (V_8C_7). FTIR spectra of the triturated powders were not particularly informative (broad band at 600 cm^{-1}) but did match authentic samples. Elemental microanalysis of the metal carbides using powdered tin as a combustion aid showed good agreement for carbon (indicating stochiometric carbides) and negligible amounts of nitrogen and hydrogen (typically $<0.2\%$). Exceptions were noted for the V_8C_7 and the TiC samples which were shown to be slightly substoichiometric in carbon (observed $V_8C_{5.63}$ and $TiC_{0.82}$). The V_8C_7 sample was investigated further by ELNES. EDX measurements on the triturated carbides showed the expected ratios of transition metal to carbon and a trace (*ca.* 2% or less) of oxygen, whilst the untriturated materials showed additionally calcium or aluminium and some chlorine corresponding to the coproduced salt. SEM of the untriturated materials showed relatively smooth particles corresponding to the formation of metal carbides with some calcium or aluminium chloride on the surface [Fig. 1(a)].

SEM of the triturated metal carbides showed agglomerates of particles of dimension 300–2000 nm typically with a faulted structure that consisted of flake like particles [Fig. 1(b)].

TEM analyses

The unusual nature of the particles found from the SEM study prompted an investigation of the microstructure of the products by TEM. To our knowledge this is one of the first TEM studies of SSM prepared particles.[3] After trituration, the products from the ampoule reactions of $TiCl_3$ and VCl_3 with Al_4C_3 at 1000 °C for 2 days and the reaction of VCl_3 with CaC_2 at 550 °C for 2 h were investigated in detail using standard imaging and diffraction techniques in a TEM.

Fig. 2(a)–(c) are dark field images of different regions of the same TiC sample. Fig. 2(a) shows an aggregate of grains of *ca.* 10 nm in size; the corresponding diffraction pattern shows that the aggregate has a polycrystalline fcc structure. Fig. 2(b) shows an aggregate of larger grains, these being *ca.* 30 nm in size. The diffraction pattern again indexes as fcc but, in this case, the crystal is textured. The observed pattern is consistent with a texture direction parallel to [022] lying close to the plane of the film. Not all of the azimuthal orientations around the texture axis are present in the diffraction pattern because the number of grains sampled was limited to only part of the agglomerate. The texture direction is indicated by an arrow on the diffraction pattern in Fig. 2(b). Although, in general, the sample consisted of aggregates of small single crystal grains, with an average grain size of 20 nm, some larger single crystal grains were also observed in the sample, one of which is shown in Fig. 2(c). Such grains were highly faulted as can be seen from the dark field image (a perfect flat uniform single crystal would exhibit uniform contrast). The diffraction

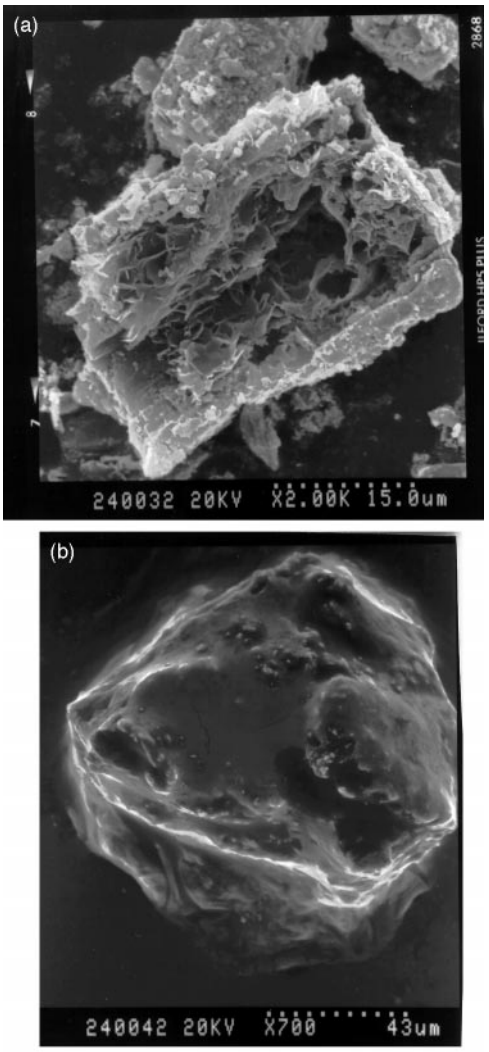

Fig. 1 (a) SEM micrograph of the product from the reaction of $TaCl_5$ and CaC_2 in air after trituration with methanol. (b) SEM micrograph of the product from the reaction of $TaCl_5$ and CaC_2 in air prior to trituration.

pattern indexes as a [111] diffraction pattern with extra spots. These extra spots are at the expected position for reflections caused by stacking faults in the fcc structure. Some traces of impurity phases were also observed in the TEM examination; these were not investigated in detail but they are likely to have been titanium oxide or carbon.

The variation in particle and crystallite sizes observed in the SSM prepared TiC is surprising. The average crystallite size observed from the X-ray line broadening studies for the TiC sample was 30 nm, and this correlated well with the average grain size observed from the TEM studies. However the TEM analysis indicates that the crystal size distribution for annealed SSM products is large and average crystallite sizes that have been extensively reported for SSM derived materials from line broadening studies should be viewed with caution.[3–5] The reason for wide variation in crystallite size could be a function of the position of the growing crystallite within the reaction mixture. It could be due to uneven heating or interdiffusion of the precursors during the SSM process or due to uneven annealing conditions. It should be noted that a high degree of faulting in the material could also lead to a broadening of the lines.

The two samples of V_8C_7 analysed in the TEM were found to be similar, containing aggregates of single crystal grains; these grains varied in size and the average grain size observed in the sample prepared using Al_4C_3 was *ca.* 100 nm whereas that in the sample prepared using CaC_2 was 20 nm. This variation in grain size can be readily accounted for due to differences in temperature (1000 *cf.* 550 °C) and annealing time (2 days *cf.* 2 h) employed in the synthesis. Most of the V_8C_7 grains observed were regular polygons [Fig. 3(a)] but some more elongated grains were also observed [Fig. 3(b)]. In V_8C_7 the metal atoms retain the positions they would have had in the NaCl structure but the C vacancies are ordered. The resulting structure is based on a supercell of eight cells of the NaCl structure. Its space group ($P4_332$ O^6) and atomic positions were determined by de Novion *et al.*[18] and Froidevaux and Rossier.[19] Fig. 4(a) shows a diffraction pattern from a single crystal grain of V_8C_7. The diffraction pattern also shows spots which are not part of the regular array. These are reflections from other crystallites within the selected area aperture. Comparison of the experimental pattern with one simulated for a [111] zone axis using the atom positions for the V_8C_7 structure shows good agreement [Fig. 4(b)]. The spots are indexed with respect to the supercell. The circled

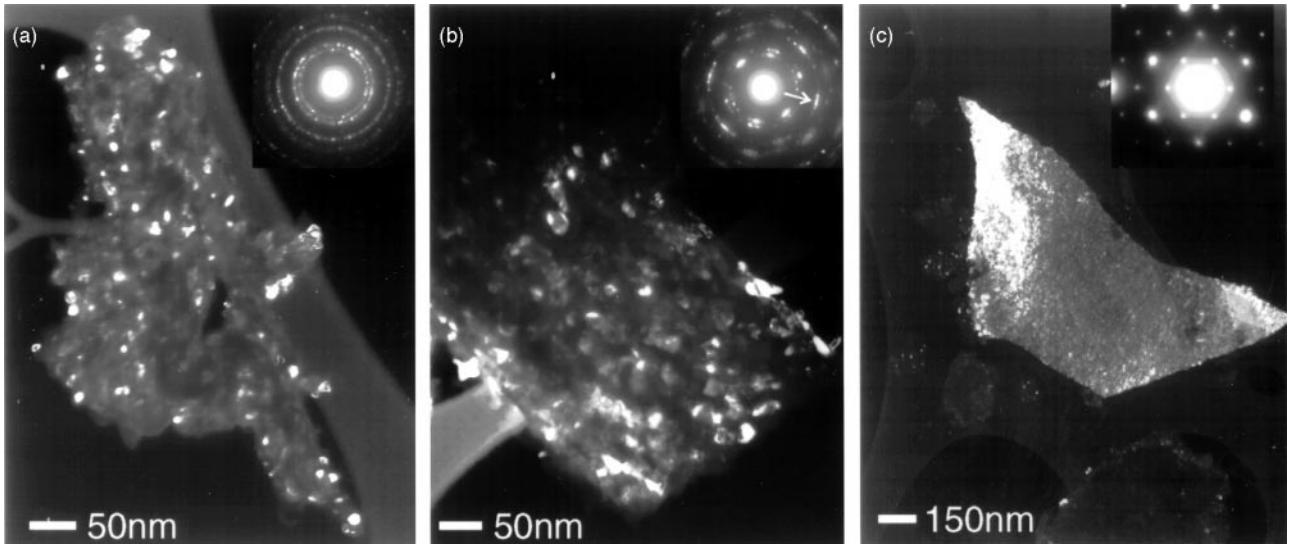

Fig. 2 TEM micrographs of the product from reaction of $TiCl_3$ and Al_4C_3. Inset images in the right hand corner represent electron diffraction maps of the particles.

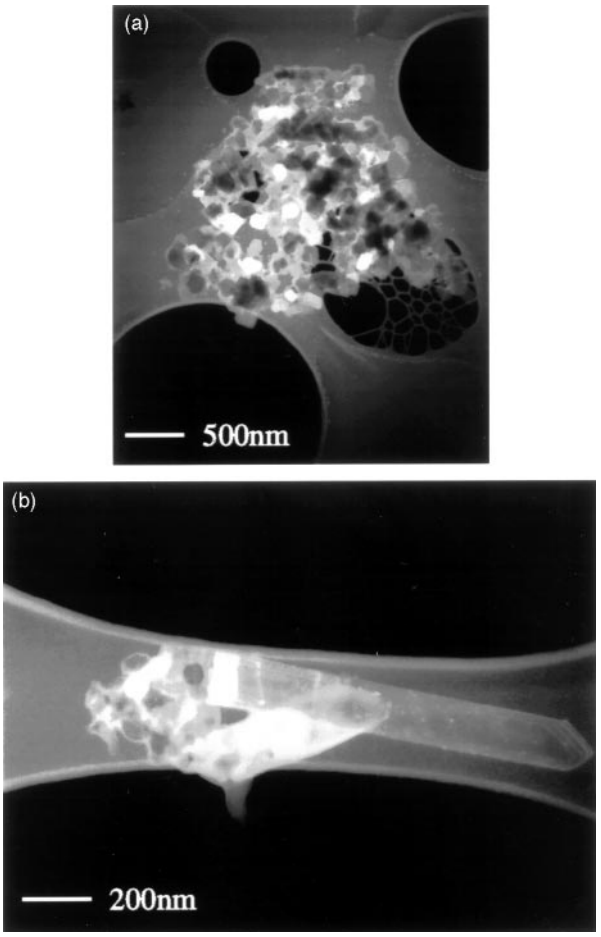

Fig. 3 TEM micrographs of the products of the reaction of VCl_3 with (a) Al_4C_3 (1000 °C, 2 days) and (b) CaC_2 (500 °C, 2 h) after trituration with methanol.

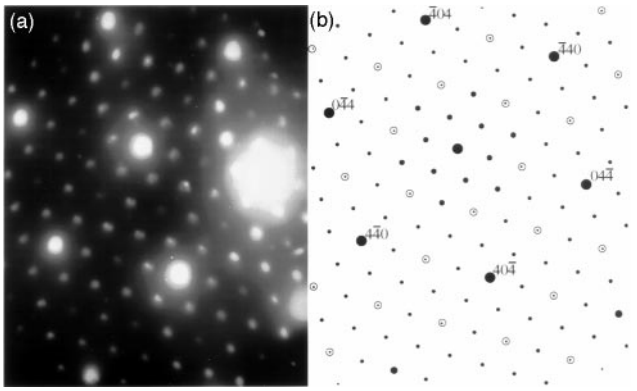

Fig. 4 (a) An electron diffraction pattern from a single crystal grain of V_8C_7. A few additional spots are present due to other small crystallites in the aperture. (b) Simulated electron diffraction pattern of V_8C_7 as determined by de Novion *et al.*[18] and Froidevaux and Rossier.[19] The pattern has a [111] zone axis. The spots in this pattern are indexed with respect to the V_8C_7 supercell.[18,19] The circled spots result from double diffraction.

spots in the simulated diffraction pattern are kinematically forbidden but occur by double diffraction and it can be seen that these spots are generally weaker in the experimental pattern. The superlattice reflections from V_6C_5[20] are at different positions to those in V_8C_7 and are not present in Fig. 4(a) (a slight C deficiency below the ideal V_8C_7 ratio would result in weak electron diffraction spots from intergrowths of V_6C_5, which would be in different positions from those observed in the experimental pattern). Thus Fig. 4 shows that the composition of the grain is close to that of the ideal V_8C_7 case. Most of the grains observed were V_8C_7 but some oxide grains were also observed. The presence of these would influence the composition determined by bulk analysis techniques. The lattice constants from all the TEM analyses were not pinpointed with precision. However they were consistent with the values obtained from the XRD studies.

X-Ray powder diffraction studies

The metal carbides isolated in the SSM reactions correspond to the most thermally stable phases.[11] Representative X-ray powder diffraction patterns are shown in Fig. 5–7. Most notable was the high degree of crystallinity that was obtained from the reaction of CaC_2 and MCl_5 (M = Nb, Ta) conducted in air over just 10 s (Fig. 5). Excess carbon precursor is present

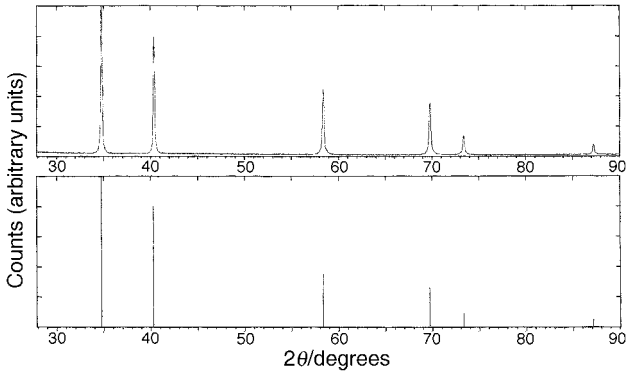

Fig. 5 Top trace; X-ray powder diffraction pattern of the product from reaction of $TaCl_5$ and CaC_2 after flame initiation in air. Bottom trace; stick pattern for TaC.

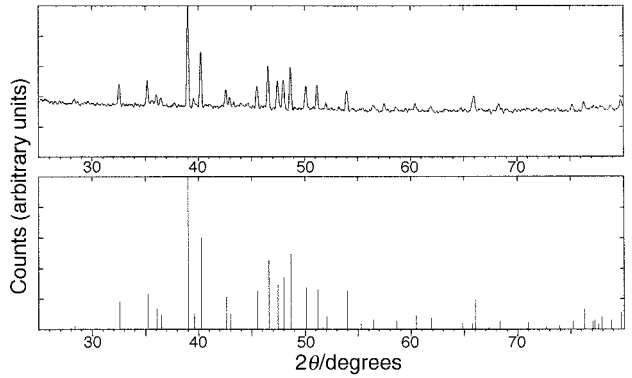

Fig. 6 Top trace; X-ray powder diffraction pattern of the product from reaction of $CrCl_3$ and Al_4C_3 at 1000 °C for 2 days. Bottom trace; stick pattern for Cr_3C_2.

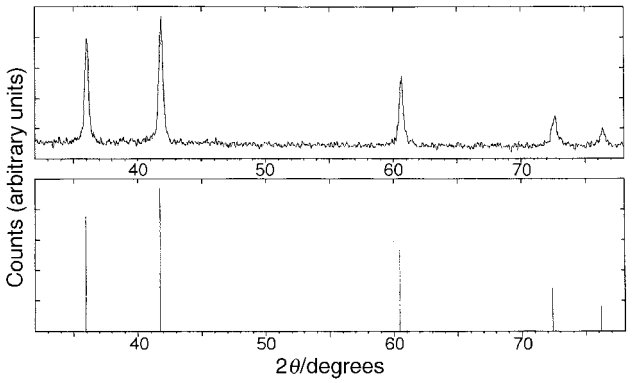

Fig. 7 Top trace; X-ray powder diffraction pattern of the product from reaction of $TiCl_3$ and Al_4C_3 at 1000 °C for 2 days. Bottom; trace stick pattern for TiC.

in all of the reactions of CaC_2. Despite this, formation of superstoichiometric phases was not observed. The lattice parameters of metal carbides have been reported to vary with degree of carbon incorporation often in a direct Vegard's law fashion.[17] This means that there is a linear relationship between the degree of non-stoichiometry and measured lattice parameter. The degree of non-stoichiometry that is tolerated in the metal carbides[11,17] before a change in phase occurs is surprising, for example the cubic rock salt structure of NbC is stable from $NbC_{1.0}$ which has a lattice parameter of $a=0.4471$ nm through to $NbC_{0.77}$ which has $a=0.4432$ nm. The reaction of $NbCl_5$ and CaC_2 produces a material with lattice parameter $a=0.4471(2)$ nm corresponding to $NbC_{1.0}$ whilst reaction of $NbCl_5$ and Al_4C_3 produces a material with parameter $a=0.4468(2)$ nm corresponding to $NbC_{0.98}$. A detailed inspection of the lattice parameters obtained from materials made by either the CaC_2 or the Al_4C_3 route indicates that in all the cubic rock salt cases the carbide matches literature values for stoichiometric ($TiC_{1.00}$, $TaC_{1.00}$) or slightly substoichiometric ($HfC_{0.75}$) products. The ZrC material appeared substoichiometric ($ZrC_{0.6}$). However the reported shift[17] in a parameter between $ZrC_{0.98}$ and $ZrC_{0.55}$ is only 0.0006 nm which is relatively small compared to the error limits of the indexing (0.0004 nm). In the molybdenum reactions, the more thermally stable hexagonal β-Mo_2C was obtained rather than cubic MoC. This may be a consequence of the exothermicity of the SSM reaction generating the most thermally stable species. The same Mo_2C phase was isolated independent of the oxidation state of the molybdenum halide precursor (Mo^{III}, Mo^{V}). The β-Mo_2C phase consists of a hexagonal close pack arrangement of molybdenum atoms with disordered carbons within the interstices. Notably the disordered form of Mo_2C was produced in the reactions rather than the ordered α-Mo_2C which has orthorhombic symmetry. In contrast, reaction of VCl_3 with CaC_2 or Al_4C_3 produced substoichiometric V_8C_7 which showed superstructure lines corresponding to ordered carbon vacancies within the structure. This correlated well with the extra electron diffraction pattern spots observed in the TEM investigation [Fig. 4(a),(b)]. The lattice parameters obtained for V_8C_7 were identical for each route and corresponded to $VC_{0.87}$ which is the highest carbon content composition for the V_8C_7 phase ($VC_{0.87}$–$VC_{0.73}$).[17]

The solid state metathesis reactions to form metal carbides tended, after the appropriate work-up procedure, to give single phase products. Only in two cases were mixed phase products identified by X-ray diffraction. Filament initiated reaction of WCl_4 and CaC_2 produced predominantly hexagonal WC but with a fraction of W_2C, whilst reaction of $MoCl_3$ and CaC_2 formed Mo_2C and Mo metal. One surprising result was the formation of nanocrystalline cubic WC from reaction of WCl_4 and CaC_2 when conducted in the presence of a diluant salt such as anhydrous magnesium chloride. In general, the cubic group 4 carbides were always less crystalline, based on X-ray line broadening,[21] than the Group 5 carbides independent of carbiding reagents or initiation conditions. Notably, for the filament or flame induced reactions in air, no metal oxide phases were detected in the products by XRD. Little difference in crystallite size as assessed by X-ray line broadening was observed between the reactions of CaC_2 and metal halides that were conducted in air for 10 s and those reactions that took place in an ampoule and were subject to annealing for two days.

Solid state metathesis routes to metal nitrides invariably form substoichiometric products that are contaminated by oxygen. The oxygen contaminants can come directly from the initial reagents, reaction vessels or indirectly from storage of the sample in air. The fine grained nature of SSM nitride products compared to traditionally prepared nitrides makes them particularly prone to oxidation.[22] We have previously reported a detailed study of CrN and Cr_2N formed by solid state metathesis with commercial materials.[21] This revealed by a combination of bulk microanalysis, lattice parameter and EELS microanalytical studies that the SSM materials had better bulk nitrogen content but equivalent or inferior microscopic composition to commercial materials. In the light of this we chose to investigate whether a similar phenomenon occurred for one of the carbide samples: V_8C_7 prepared from reaction of Al_4C_3 and VCl_3. This study, which we have briefly communicated upon previously,[9] showed the expected carbon and vanadium edges in the EELS. The concentration of oxygen was difficult to determine because of the overlapping vanadium and oxygen edges. However, by subtracting the vanadium edge shape in the absence of oxygen from that of the sample, the oxygen content was shown to be <3 atom%.[23] This indicates that the SSM prepared carbides are not as susceptible to oxidation as SSM prepared metal nitrides.

Thermodynamic considerations

Solid state metathesis reactions are driven primarily by the lattice energy of the coproduced salt. Reactions are often energetic enough to sustain a synthesis wave through the material from a point source of initiation. Ease of spread of the synthesis wave is dependent on the exothermicity of the reaction and the melting points of the coproduced salts. If the reaction is sufficiently exothermic, it can spread as the reaction front ignites successive layers of reactants.[5] Solid state metathesis reactions can also be made to occur in reactions that are weakly exothermic without the spread of a synthesis wave provided that they are heated externally.[5] In the reactions to produce metal carbides, the reactions involving CaC_2 did proceed with a synthesis wave whilst those using Al_4C_3 required extensive heating in a furnace. Hesse's law calculations[5] for TiC formation from CaC_2 and $TiCl_3$ [eqn. (5)] show the reaction has an exothermicity of -530 kJ mol^{-1} whilst reaction of Al_4C_3 with $ZrCl_4$ has an exothermicity of -100 kJ mol^{-1} [eqn. (6)].

$$3/2CaC_2 + TiCl_3 \rightarrow TiC + 3/2CaCl_2 + 2C \quad (5)$$

$$\Delta H_{react} = -530 \text{ kJ mol}^{-1}$$

$$ZrCl_4 + 1/3\ Al_4C_3 \rightarrow ZrC + 4/3AlCl_3$$

$$\Delta H_{react} = -100 \text{ kJ mol}^{-1} \quad (6)$$

These exothermicities correlate well with observations made during the SSM reactions to form metal nitrides where the more exothermic reactions ($\Delta H_{react} = -400$ kJ mol^{-1}) were able to propagate whilst the less exothermic reactions ($\Delta H_{react} = -200$ kJ mol^{-1}) required heating in an ampoule. The critical quantity in determining the ease of reaction propagation has been empirically determined as $T_{ad,s}$ the adiabatic reaction temperature reached in the reaction for salt formation only (here $3CaC_2 + 2TiCl_3 \rightarrow 2Ti + 6C + 3CaCl_2$). If $T_{ad,s}$ equals or exceeds the melting point of the coproduced salt the reaction will propagate.[5] In the CaC_2 reactions $T_{ad,s}$ exceeds 782 °C, the melting point of $CaCl_2$, and the reaction propagates with a synthesis wave whilst for the Al_4C_3 reactions $T_{ad,s}$ is actually below room temperature.

The ease of reaction initiation in SSM reactions is related to the solid state diffusion barrier. Reactions in which one of the components undergoes a phase change either by melting, subliming or changing structure stimulates the SSM process and allows reaction propagation.[3] Reactions involving CaC_2 had all initiated by 350 °C. In the case of $NbCl_5$ and $TaCl_5$ with CaC_2 the initiation temperature for ampoule reactions was noted at 230 °C and corresponded to the melting points of the initial halides. In the other systems the initiation temperature correlated with a CaC_2 phase change. Al_4C_3 reactions tended to occur at temperatures just below the melting points of the starting transition metal halide. As has been noted above, the Al_4C_3 reactions did not proceed with a

synthesis wave and were thermally driven by heating in an evacuated quartz ampoule. The degree of crystallinity of the product in the Al_4C_3 reactions was unsurprisingly related to annealing time. However, the reactions could be stopped after heating at 800–1000 °C for 1 h and seemed to have gone to completion, giving after trituration, single phase metal carbides. The XRD patterns after 1 h could be indexed as those from the standard crystal structure but the widths of the reflections indicated that the crystallite sizes were about half of that from the annealed product.

Reaction mechanism

Solid state metathesis reactions have been speculated to proceed by two pathways either reductive recombination or ionic metathesis. In reductive recombination the reaction occurs *via* reduction to the elements followed by recombination [eqn. (7)].[5] Ionic metathesis involves the exchange of ions within the melt of coproduced salt [eqn. (8)].

$$3ZrCl_4 + Al_4C_3 \xrightarrow{\text{reduction}} 3Zr + 3C + 4\ AlCl_3$$

$$\xrightarrow{\text{recombination}} 3ZrC + 4\ AlCl_3 \qquad (7)$$

$$3ZrCl_4 + Al_4C_3 \rightarrow 3Zr^{4+} + 3C^{4-} + 4\ AlCl_3 \rightarrow 3ZrC + 4\ AlCl_3 \qquad (8)$$

Formation of metal nitrides by solid state metathesis reaction has been identified as proceeding by both pathways. Formation of TiN by a filament initiated SSM reaction also produces some Ti metal, indicating a reductive recombination route.[6] Formation of LaN from reaction of $LaCl_3$ and Li_3N involves intermediates of the form La_2Cl_3N indicating an ionic pathway.[5] In no case were intermediates observed in the reaction of Al_4C_3 and metal halides. Neither was any metal found in the product. The reaction is partially encouraged by the formation of a melt of $AlCl_3$. However, the temperature gradients within the reaction ampoule and temperatures required for carbide formation meant that most of the $AlCl_3$ sublimed away from the reaction site. The reaction could be speculated as an ionic metathesis with the provision that the ions that are exchanging are not necessarily, as in the case of eqn. (8), Zr^{4+} and C^{4-}. In the reactions of CaC_2 and metal halides, the reaction does not proceed by a formal ionic metathesis. CaC_2 consists of calcium ions and acetylide units (C_2^{2-}). At no point was a transition metal product isolated which contained a diacetylide unit. It can be hypothesised that the acetylide carbons may undergo a disproportionation reaction in forming transition metal carbides and coproduced carbon.

Reaction scope

Reaction of Al_4C_3 or CaC_2 with transition metals from groups 4, 5 and 6 produces transition metal carbide products. Reaction of yttrium halide or lanthanum halide with either Al_4C_3 or CaC_2 in a sealed ampoule for 2 days at 800 °C did not produce yttrium or lanthanum carbide, only unreacted starting materials. Carbides for these two elements are well known and characterised. Reaction of the later transition metal halides with CaC_2 and Al_4C_3 also failed to produce carbide products and formed the metals Cu, Ni and Co. In the reaction of iron trichloride and Al_4C_3, Fe_3C is formed as the primary product.

The phases isolated by the solid state metathesis reactions for the formation of metal carbides mirror those phases isolated by SSM reactions to form nitrides. In both cases, a barrier termed the chromium enigma[23] stops isolation of carbide or nitride products much beyond group 6. In both cases, this can be related to the thermal instability of the ME and M_2E (E = C, N) phases of the later transition elements. In these cases the decomposition temperatures of the nitrides and carbides are below the synthesis wave (*ca.* 1100 °C) or oven temperatures used in the reaction.

Typically the scale of these metathesis reactions to produce metal carbides has been kept on the order of gram quantities. Scale-up of the reaction to multigram quantities has proven successful in all the cases tried (NbC, TaC). It would be difficult to envisage producing kilogram quantities of metal carbides from these reactions because of the air sensitivity of the reagents, however we have shown previously that it is possible to form multikilogram quantities of $BaTiO_3$ by metathesis reactions from air-sensitive reagents.

Conclusions

Solid state metathesis reactions of CaC_2 and metal halides offer a fast (10 s) exothermic method for the formation of crystalline metal carbides. Transition metal carbides can also be made in sealed ampoule reactions of anhydrous transition metal chlorides and Al_4C_3 (1000 °C) or CaC_2 (350 °C). Carbide products could be isolated from the reactions within 1 h although typically the Al_4C_3 products were annealed for 2 days. CaC_2 reactions proceeded with a synthesis wave whilst the Al_4C_3 reactions did not. The ease with which a synthesis wave formed in the reactions could be related to $T_{ad,s}$ the adiabatic temperature for salt formation only. The metal carbides formed in all the reactions corresponded primarily to stoichiometric or just substoichiometric materials and always formed the most thermally stable modification. SSM reactions work well for all of the early transition elements from groups 4, 5 and 6. For the later transition metals the reactions produce the metal. TEM investigations of the carbides formed by solid state metathesis show a wide crystallite size distribution within the same sample.

Experimental

All reagents were of 99.9% purity or better, purchased from Aldrich Chemical Co. and used without further purification. Manipulations and weighings were carried out in a Saffron Scientific nitrogen filled glove box. Ampoules were made from quartz or Pyrex (1 cm diameter, 20 cm long) and sealed with the reactants under vacuum. X-Ray powder diffraction patterns were determined on a Siemens D5000 transmission powder diffractometer using germanium monochromated Cu-Kα1 radiation ($\lambda = 1.5046$ Å). Patterns were indexed using TREOR or METRIC—LS programmes. SEM/EDX was determined on a JEOL JSM820 microscope, equipped with a Kevex Quantum Detector Delta 4, and a Hitachi SEM S-570. IR spectra were recorded on a Nicolet 205 spectrometer using KBr pressed discs. Elemental compositions were determined by the departmental service using combustion in oxygen with tin powder as a combustion aid. The EELS spectra from the commercial VC powder (Alpha chemicals) were recorded using a GATAN 666 PEELS spectrometer on a VG Microscopes HB5 scanning transmission electron microscope operated at 100 keV while those from the V_8C_7 produced by the SSM reaction were recorded using a similar spectrometer system on a Philips CM20 transmission electron microscope with a field emission gun operated at 200 keV. Electron diffraction and TEM investigations of SSM prepared TiC and V_8C_7 were performed on a JEOL 1200EX or a JEOL 2000FX microscope. Samples for EELS and TEM were prepared by crushing the SSM powders in propan-2-ol, using a pestle and mortar, and dispersing onto a holey carbon film on a Cu grid.

Reactions of Al_4C_3 and transition metal halides ($TiCl_3$, $ZrCl_4$, $HfCl_4$, VCl_3, $NbCl_5$, $TaCl_5$, WCl_4, $MoCl_3$ and $MoCl_5$)

Transition metal halide, MX_n, and aluminium carbide, $(n/12)Al_4C_3$ (0.1 mmol), were ground together and heated

inside an evacuated ampoule. The ampoule was placed with 2/3 of its length inside a tube furnace at 500 °C. The reaction was left for 2–3 h at 500 °C and then the temperature was raised by 100 °C every 12 h to 1000 °C and left to anneal for 2–5 days. The coformed $AlCl_3$ separated from the black–grey carbide product by sublimation to the cool end of the ampoule.

The black or grey solids obtained were treated with THF (2×5 ml), methanol (1×10 ml) and dried *in vacuo*. The resulting grey to black powders were analysed using powder XRD (Table 1), SEM/EDX, FTIR, elemental microanalysis and in the case of V_8C_7 EELS and for TiC and V_8C_7 TEM and electron diffraction measurements. [Microanalysis: V_8C_7: found: C, 13.75; H, 0.21; N, 0.19. Calc.: C, 17.07%; Mo_2C: found: C, 6.66; H, 0.0; N, 0.0. Calc.: C, 5.88%; WC: found: C, 6.64; H, 0.14; N, 0.0. Calc.: C, 6.12%; NbC: found: C, 11.30; H, 0.0; N, 0.0. Calc.: C, 11.43%; TiC: found C, 16.47; H, 0.06; N, 0.11. Calc.: C, 20.03%. Theoretical percentages were determined assuming the products were fully stoichiometric. Quantitative EDAX analysis of the metal carbide products invariably showed at least 98% metal carbide with stoichiometric M/C ratios.]

Ampoule reactions of CaC_2 with $TiCl_3$, $ZrCl_4$, VCl_3, WCl_4, $NbCl_5$, $TaCl_5$, $MoCl_3$ and $MoCl_5$

Metal halide, MX_n, and calcium carbide, $(n/2)CaC_2$ (0.2 mmol), were ground together and heated in an evacuated Pyrex glass ampoule. This induced a rapid reaction which produced a red glow at *ca.* 200–350 °C with the product spread along the inside walls of the ampoule. The temperature was ramped to 500 °C, left for an hour and allowed to cool to room temperature. The solids obtained were triturated with methanol (5×6 ml), dried *in vacuo* and analysed by powder XRD (Table 1), SEM/EDX and FTIR. (Microanalysis: NbC; found: C, 11.13; H, 0.16; N, 0.11. Calc.: C, 11.43%.)

Flame initiated reactions of CaC_2 with $TiCl_3$, $ZrCl_4$, VCl_3, WCl_4, $NbCl_5$, $TaCl_5$, $MoCl_3$ and $MoCl_5$

Metal halide, MX_n, and calcium carbide, $(n/2)CaC_2$ (0.2 mmol), were ground together. The resulting powder was placed inside a ceramic boat in air. A reaction was initiated in the powder by application of a flame from a gas torch at *ca.* 1000 °C. This induced an orange flame that moved through the solid to leave a black partly fused powder. The solids obtained were triturated with methanol (5×6 ml), dried *in vacuo* and analysed by powder XRD (Table 1), SEM/EDX and FTIR.

Acknowledgements

The authors thank the EPSRC for grants GR/L06850 and GR/K93600.

References

1 Z. A. Munir, *Ceram. Bull.*, 1988, **67**, 342.
2 A. G. Merzhanov, *J. Mater. Proc. Technol.*, 1996, **56**, 222.
3 I. P. Parkin, *Chem. Soc. Rev.*, 1996, 199.
4 E. G. Gillan and R. B. Kaner, *Chem. Mater.*, 1996, **8**, 333.
5 J. C. Fitzmaurice, A. Hector and I. P. Parkin, *J. Chem. Soc. Dalton Trans.*, 1993, 1569; J. C. Fitzmaurice, A. L. Hector and I. P. Parkin, *Polyhedron*, 1993, **12**, 1295; A. T. Rowley and I. P. Parkin, *Adv. Mater.*, 1994, **6**, 780; A. L. Hector and I. P. Parkin, *Chem. Mater.*, 1995, **7**, 1222; A. Hector and I. P. Parkin, *Polyhedron*, 1995, **14**, 913; S. Ali, M. Aguas, A. Hector, G. Henshaw and I. P. Parkin, *Polyhedron*, 1997, **16**, 2635; E. G. Gillan and R. B. Kaner, *Inorg. Chem.*, 1994, **33**, 5693; L. Rao and R. B. Kaner, *Inorg. Chem.*, 1994, **33**, 3210; R. E. Treece, G. S. Macala, L. Rao, D. Franke, H. Eckert and R. B. Kaner, *Inorg. Chem.*, 1993, **32**, 2745.
6 C. H. Wallace, S. H. Kim, G. A. Rose, L. Rao, J. R. Heath, M. Nicol and R. B. Kaner, *Appl. Phys. Lett.*, 1998, **72**, 596; L. Rao and R. B. Kaner, *Inorg. Chem.*, 1994, **33**, 3210; E. Ponthieu, L. Rao, L. Gengembre, J. Grimbolt and R. B. Kaner, *Solid State Ionics*, 1993, **63**, 116.
7 J. C. Fitzmaurice, A. Hector, I. P. Parkin and A. T. Rowley, *Polyhedron*, 1994, **13**, 235; I. P. Parkin and A. T. Nartowski, *Polyhedron*, 1998, **17**, 2617.
8 J. C. Fitzmaurice and I. P. Parkin, *New J. Chem.*, 1994, **18**, 825; *J. Mater. Sci. Lett.*, 1994, **13**, 1185.
9 I. P. Parkin, A. T. Nartowski, A. Craven and M. MacKenzie, *Adv. Mater.*, 1998, **10**, 805; S. R. Holm and R. B. Kaner, *Abstr. Am. Chem. Soc.*, 1997, **213**, 151.
10 P. Ettymayer and W. Lengauer, in *Encyclopedia of Inorganic Chemistry*, ed. R. B. King, J. Wiley, Chichester, 1994, vol. 2, p. 519.
11 *Kirk–Othmer Encyclopedia of Chemical Technology*, ed. J. L. Kroschwitz, 4th edn., J. Wiley and Sons, Chichester, 1992, vol. 4, p. 841; A. Neckel, *The Physics and Chemistry of Carbides, Nitrides and Borides*, ed. R. Freer, Kluwer, Dordrecht, 1990, p. 458; K. J. A. Brookes, *World Directory and Handbook of Hard metals and Hard Materials*, International Carbide data, East Barnet, Hertfordshire, UK, 5th edn., 1992.
12 S. P. Murarka, *Defect Diffus. Forum*, 1988, **59**, 99.
13 C. J. Terry and J. D. Frank, *US Pat.*, 4834963, 1989.
14 P. M. McKenna, *US Pat.*, 2529778, 1950.
15 K.-H. Habig, *J. Vac. Sci. Technol. A*, 1976, **4**, 2832.
16 S. T. Oyama, *J. Solid State Chem.*, 1992, **96**, 1; S. T. Oyama and G. L. Haller, *Catalysis*, *Specialist Periodical Reports*, The Royal Society of Chemistry, London, 1982, vol. 5, p. 333.
17 H. Goldsmidt, *Interstitial Alloys*, Butterworths, London, 1967, p. 92.
18 C. H. de Novion, R. Lorenzelli and P. Costa, *C. R. Hebd. Séances Acad. Sci. Paris*, 1966, **263**, 775.
19 D. Froidevaux and D. Rossier, *J. Phys. Chem. Solids*, 1967, **28**, 1197.
20 J. D. Venables, D. Khan and R. G. Lye, *Philos. Mag.*, 1968, **8**, 177.
21 H. P. Klug and L. E. Alexander, *X-Ray Diffraction Procedure for Polycrystalline and Amorphous Materials*, J. Wiley, 2nd edn., New York, 1974.
22 M. D. Aguas, A. M. Nartowski, I. P. Parkin, M. MacKenzie and A. J. Craven, *J. Mater. Chem.*, 1998, **8**, 1875.
23 A. J. Craven, *J. Microsc.*, 1995, **180**, 250.
24 L. E. Toth, *Transition Metal Carbides and Nitrides*, Academic Press, New York, 1971.

Paper 8/08642G